Available online at www.sciencedirect.com
ScienceDirect
Trans. Nonferrous Met. Soc. China 23(2013) 3770−3779
Transactions of Nonferrous Metals Society of China
www.tnmsc.cn

Water leaching kinetics and recovery of potassium salt from sintering dust

Guang ZHAN, Zhan-cheng GUO
State Key Laboratory of Advanced Metallurgy, University of Science and Technology Beijing, Beijing 100083, China

Received 27 February 2013; accepted 13 April 2013

Abstract: Surface morphology and inner structure of the dust were observed by ICP-AES, SEM-EDS and XRD to examine the strengthening measures of leaching potassium salt from the sintering dust by water. The results showed that the main component of the sintering dust was iron−oxygen compound, with KCl adsorbed on its surface. Leaching experiments showed that the KCl in the ESP dust could be separated and recovered by water leaching and fractional crystallization. The yield of K−Na vaporized crystalline salt was 18.56%, in which the mass fractions of KCl, NaCl, $CaSO_4$ and K_2SO_4 were about 61.21%, 13.40%, 14.62% and 10.86%, respectively. The leaching kinetics of potassium salt from the sintering dust fits the external diffusion model well. The leaching speed and the leaching rate of the potassium salt can be increased by increasing the leaching temperature, strengthening the stirring speed and increasing the liquid−solid ratio.

Key words: potassium salt; sintering dust; leaching kinetics; intensified leaching

1 Introduction

Potash, an essential fertilizer for crop growth, is very important for China, which feeds 22% of people on earth with less than a tenth of the world's arable land. In the first ten months of 2012, the potash fertilizer imports in China increased by 9.7% to 5.714 million tons (pure KCl) [1,2] and the CFR (cost and freight) price increased by 23.7% to 470 dollars per ton [3]. The main reasons for the increasing price of the potash were the increase of the consuming capacity of potash fertilizer as well as the decrease of its production in China. The reason for the price of the potash soaring up is that the consuming capacity of potash fertilizer in China is rising whilst its production is shrinking, which is mainly attributed to the limited reserves, the backward technology with complex procedures, the low production capacity (only 4.8 million tons per year, pure K_2O), and the geographic location too remote, inconvenient traffic and very harsh climate [1,4,5].

Sintering dust generated during the steel-making sintering process and collected by electrostatic precipitator, is usually considered a kind of solid waste. It is considered a dangerous dust because of its complicate components such as heavy metals and hazardous components [6]. A usual way to treat the sintering dust is returning it to the sintering furnace to reuse Fe and C. However, great amount of other elements such as, K, Na, Zn and Pb are also reused in the recycle, which is harmful for normal operation of blast furnace and sintering machine [7−12]. Thus, it is necessary to study new technologies for its processing. It is obtained that the mass contribution of KCl is up to 30%, some even up to 40% in the dust. Statistically, there is approximate 4 kg of this kind of dust produced per ton steel [13]. So, it is a considerable number of the total amount of this dust, which contains 0.84 million tons of KCl in 2012 (calculating with KCl content of 30%) [14].

Based on a large number of experiments [15,16], a national invention patent of producing potassium chloride from sintering dust was applied by GUO et al [17], and a potassium chloride plant with a capacity of 10000 t/a sintering dust was built in Tangshan, China. The simplified potassium recovery process shown in Fig. 1 was designed as follows: leaching the sintering dust with water at a certain temperature (step 1); and filtering the leaching solution after some time (step 2); then removing heavy metal impurities from the filtrate and recycling the residue as iron ore concentrate (step 3); finally, evaporating the purified filtrate step by step to obtain the high purity products (step 4).

Foundation item: Projects (2012AA062502, 2012AA06A118) supported by the High-tech Research and Development Program of China
Corresponding author: Zhan-cheng GUO; Tel/Fax: +86-10-82375042; E-mail: zcguo@metall.ustb.edu.cn
DOI: 10.1016/S1003-6326(13)62928-3

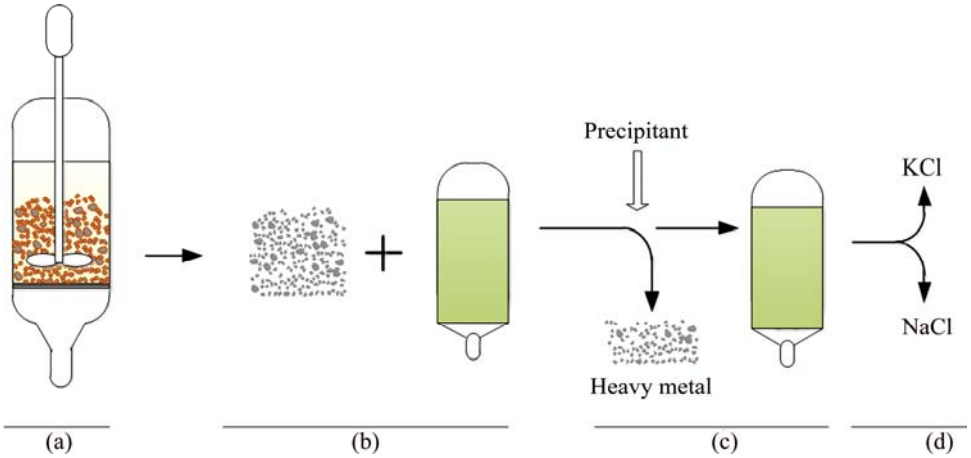

Fig. 1 Process flow diagram of recycling potassium resource: (a) Leaching process; (b) Filtration process; (c) Impurity removal process; (d) Separation process

In order to expand the applying scope of the new technology, the physical properties of different metallurgical dusts should be investigated. Furthermore, a theoretical model about controlling the production process can be built by studying the leaching kinetics in depth, which could be helpful to improving the leaching effects.

PENG et al [13] derived a leaching kinetic formula for sintering dust by the linear relationship between the concentration and electrical conductivity of the leaching solution. However, in their research, the liquid−solid ratio was enlarged to 100/1 without considering the actual situation. So, the obtained linear relationship cannot reflect the actual leaching behaviour of potassium from the sintering dust. In this work, the sintering dust collected from Baotou Steel (Group) Corporation was studied. The physicochemical properties of the dust, the leaching mechanisms, the leaching kinetic model and the intensifying leaching methods were studied in detail. This work is intended to obtain a more practical theoretical model for controlling the production process.

2 Experimental

2.1 Sample component analysis

An ESP dust sample from Baotou Steel (Group) Corporation was subjected to chemical analysis to determine the mass contribution of potassium. On one hand, the mineral elements of the ESP dust were detected using an X-ray fluorescence spectrometer (XRF−1800, Japan). On the other hand, the composition of the dust sample was analyzed by the following method: the sample was mixed with an acid mixture ($V(HNO_3)$:$V(HClO_4)$:$V(HF)$=5:3:2) in a polytetrafluoroethylene beaker and placed in a high-pressure digestion oven at 170 °C for 5 h. The digested acid mixture was analyzed with an ICP-AES (Perkine-Elmer OPTIMA 3000, USA) to measure the concentrations of the trace elements (Al, Ca, Fe, K, Mg, Na, Pb, Si and Zn).

2.2 Existing state of K element in dust

The structural characterization of ESP dust and its filter residue obtained after water leaching was performed by an X-ray diffraction analyzer (M21, MAC, Japan). Samples of the dust were examined under a scanning electron microscope (SEM) (Cambridge S−360, UK) and X-ray mapping (Tracor Northern, USA) via SEM-EDS to gain a better understanding of the ESP dust. The prepared samples were subjected to the X-ray mapping via SEM-EDS for elements Cl, K, Na, Fe, Ca, S and O.

2.3 Water leaching experiments

4.9839 g of ESP dusts were added into 100 mL deionized water in a conical flask and stirred for 10 min. After being filtrated, the residue was leached with another 100 mL deionized water at least 4 times. The combined filtrate was collected and evaporated to crystals. The concentrations of the major water-soluble particle species (K^+, Na^+, Ca^{2+}, Mg^{2+}, Al^{3+}, Cl^-, SO_4^{2-}, NO_3^-, Br^-, F^-, and PO_4^{3-}) in the crystals were determined by an ICP−AES and IC ion chromatograph (Metrohm 792 Basic, Switzerland). The structural characterization of the crystal substance was performed by X-ray diffraction analysis.

3 Results and discussion

3.1 Sample component

The ICP-AES result of the digested acid mixture is shown in Table 1. The result shows that main metal constituents of the ESP dust are iron (37.92%), potassium (6.89%) and calcium (6.76%), indicating that this ESP dust is ferric oxide with a high concentration of potassium and calcium. It is worthy to be noted that the contribution of K is high in the dust.

Table1 ICP-AES results of ESP dust (mass fraction, %)

TFe	K	Si	Zn	Ca	Al	Na	Mg	Pb
37.92	6.89	13.69	0.83	6.76	1.31	2.82	1.75	3.62

3.2 Existing state of K element in dust

Figure 2 shows the X-ray diffraction pattern of the ESP dust. Clearly, the major constituents in the ESP dust are KCl, NaCl, Fe_2O_3 and Fe_3O_4. The strong diffraction peaks of potassium chloride illustrate its high content in the ESP dust. These results are identical with the data obtained by the ICP-AES analysis. Potassium is more volatile than other metal elements in this study. Therefore, potassium compounds volatilized in the sintering process and then were condensed into particles. The SEM-EDS result in Fig. 3 shows further proof of the presence of KCl particles in the ESP dust. The X-ray mapping of the elements K and Cl shows that the particle at point 1 is the KCl particle, which is adsorbed on the iron oxide compound. It is clear to see that the potassium exists mainly in the form of KCl in the ESP, therefore Cl and K always have the same distribution.

The sintering dusts were analyzed by ICP-AES and XRD. The main composition and XRD patterns of the different particle sizes of sintering dusts are shown in in Table 2 and Fig. 4, respectively. It indicates that the particle size distribution of the sintering dust is main below 0.15 mm (75.61%) and the potassium content increases with the decreasing particle size.

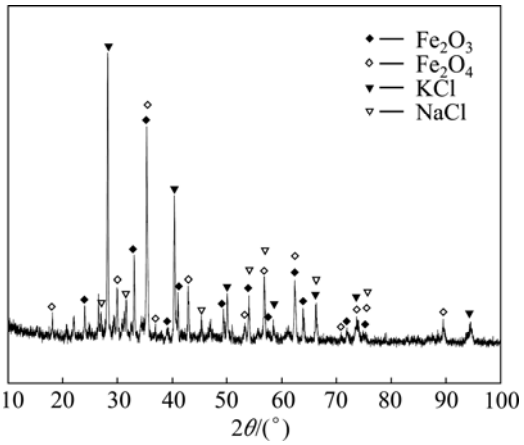

Fig. 2 XRD pattern of ESP dust

3.3 Water leaching

In order to discuss the possibility of potassium recycling, a water leaching experiment was carried out on the sintering dust (section 2.3). After the water leaching and evaporative crystallization, 18.56% K−Na salt can be recovered. Figure 5 shows the X-ray diffraction pattern of the water-washed ESP dust. After water leaching, the KCl and NaCl were dissolved in water and the peaks of these phases in the XRD pattern disappeared accordingly. The main components of the residue are Fe_2O_3 and Fe_3O_4. That is to say, the water-soluble potassium can be separated from the sintering

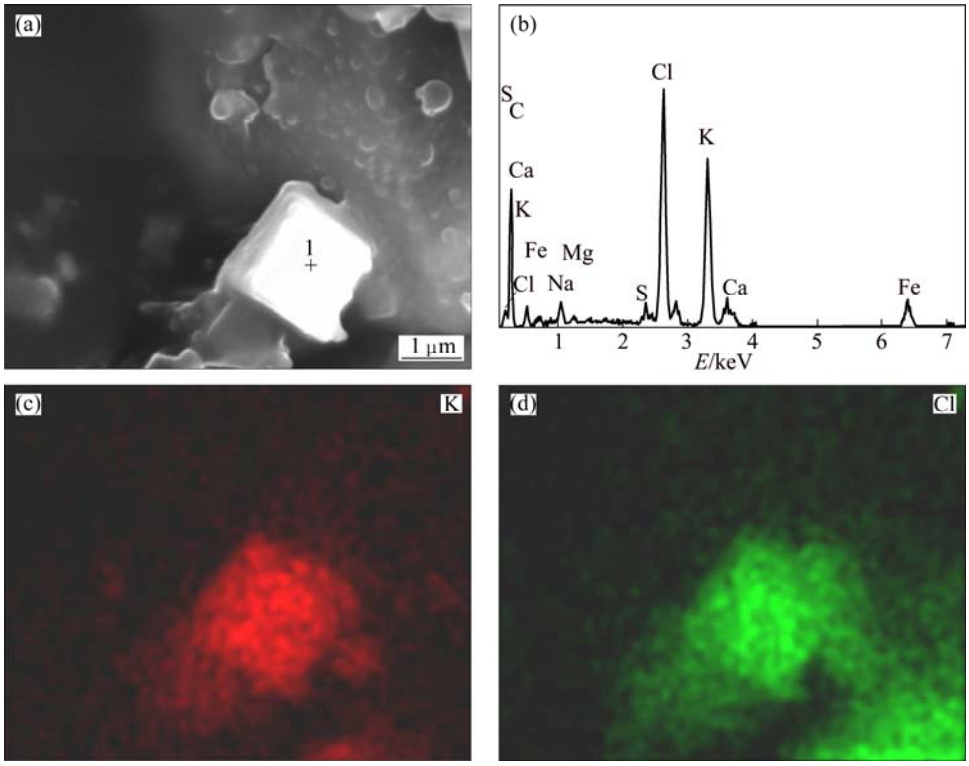

Fig. 3 SEM-EDS mapping of K and Cl for ESP dust particle: (a) SEM image; (b) EDS result of point 1 in (a); (c) EDS mapping of K; (d) EDS mapping of Cl

Table 2 ICP-AES results of sieved sintering dust

Element	Mass fraction/%				
	>0.5 mm (2.54%)	0.25−0.5 mm (5.9%)	0.15−0.25 mm (15.95%)	0.075−0.15 mm (45.14%)	<0.075 mm (30.47%)
K	4.61	5.61	6.94	8.34	9.08
Zn	0.46	0.25	0.08	0.74	$7.9*10^{-3}$
Ca	6.69	6.08	5.74	4.62	3.8
Al	0.84	0.81	0.81	0.67	0.55
Na	1.13	0.8	1.06	1.55	1.26
Mg	1.75	1.58	1.58	1.48	1.04
Pb	0.41	0.66	1.07	1.54	1.74
As	0.11	2.55×10^{-2}	–	–	–
Cu	0.19	0.18	0.19	0.19	0.19
Fe	49.19	46.32	42.99	44.49	47.41
Si	1.53	1.49	0.32	0.27	0.61

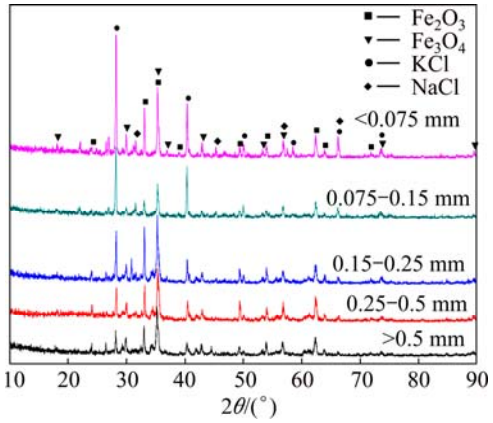

Fig. 4 XRD patterns of sieved sintering dust

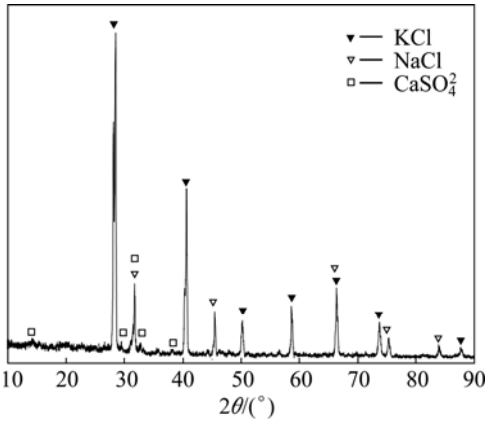

Fig. 6 XRD pattern of crystal substance

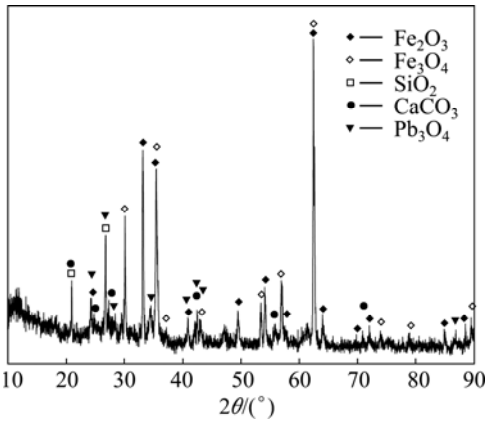

Fig. 5 XRD pattern of water-washed dust

dust easily through water leaching which makes the recovery of potassium resource possible.

The XRD analysis of the crystals (Fig. 6) and SEM-EDS mapping (Fig. 7) show the presence of KCl and NaCl with a small amount of $CaSO_4$ and K_2SO_4. It can be inferred that point 1 represented mainly NaCl and KCl crystal and point 2 presented mainly $CaSO_4$ and K_2SO_4 crystal. From the results of element analysis of crystals (Table 3), it is known that only K^+, Ca^{2+}, Na^+, Cl^- and SO_4^{2-} ions present in the crystal substance with mass fraction as follows: 61.21% KCl, 13.4% NaCl, 14.62% $CaSO_4$ and 10.86% K_2SO_4. This is to say, more than 97% potassium in the dust has been extracted out except the other small proportion left as aegirite and riebeckite which are generally indissolvable [18].

3.4 Leaching kinetics

The kinetic equations regarding leaching experiments usually reflect the functional relationship between the leaching rate and the leaching time. Therefore, the effective measures can be taken to increase the leaching rate according to the calculated kinetics parameters and activation energy which can reflect the rate-limiting step in the leaching process [19−21].

Under the same conditions of stirring speed 300 r/min, liquid−solid ratio 5:1 (mL/g), and leaching time 60 min, the K^+ concentrations of the leaching solution at leaching temperatures ranging from 20 °C to 60 °C were detected. The effect of leaching temperature on the leaching rate of K^+ is shown in Fig. 8. It can be seen that the lower the leaching temperature is, the more slowly the leaching equilibrium achieved. The leaching rate of

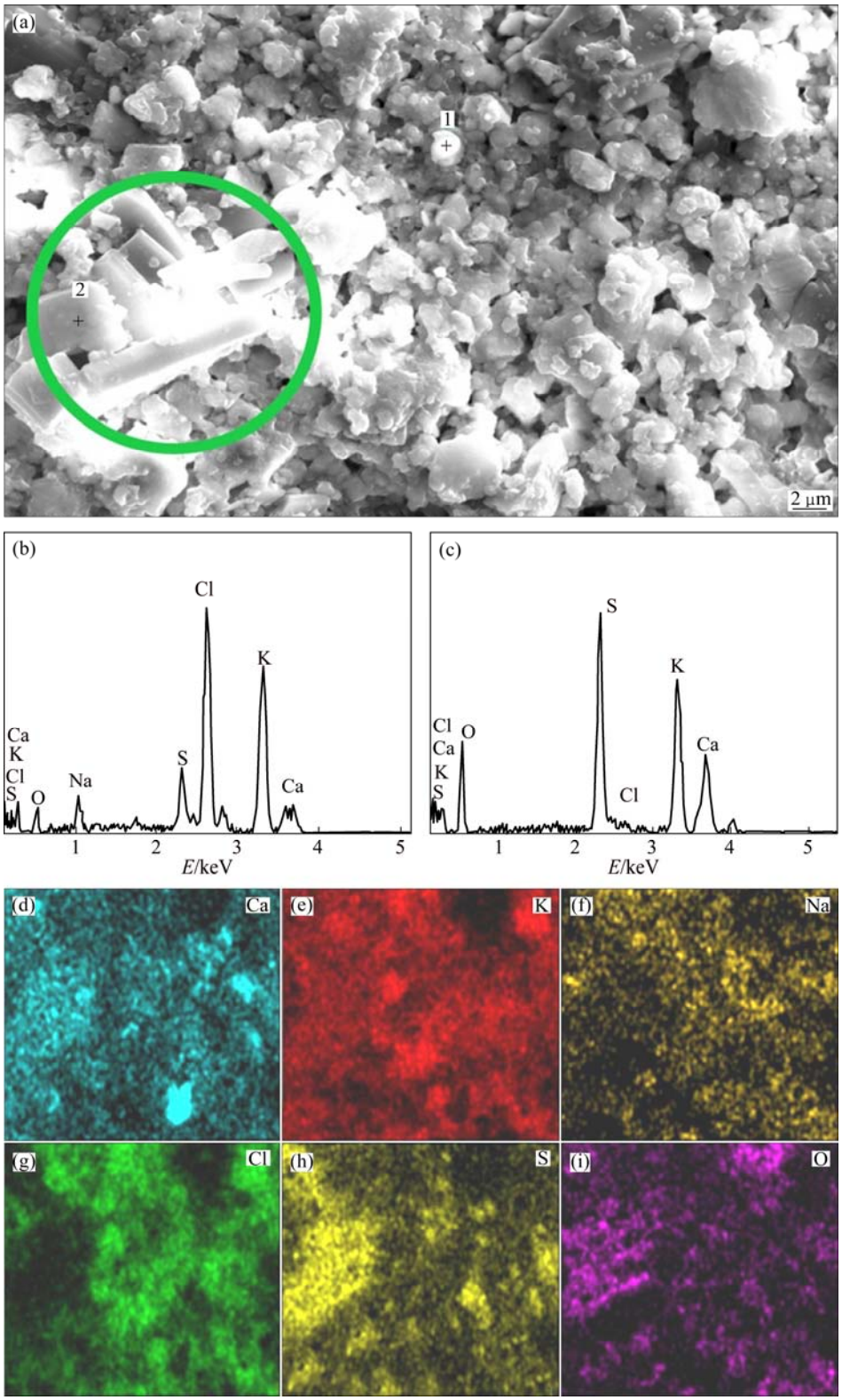

Fig. 7 SEM-EDS mapping of crystal substance: (a) SEM image; (b) EDS result of point 1; (c) EDS result of point 2; (d) EDS mapping of Ca; (e) EDS mapping of K; (f) EDS mapping of Na; (g) EDS mapping of Cl; (h) EDS mapping of S; (i) EDS mapping of O

K^+ reached 90% and the leaching equilibrium time was about 180 s at 20 °C. It was found that until 60 °C, with temperature increasing, the leaching speed and the leaching rate improved rapidly; however, with temperature continuing rising, the increase in leaching rate became slow. A possible reason for this is that, in the beginning the rising temperature made diffusion rate speed up so the leaching speed got faster, whilst after

Table 3 ICP-AES and IC results of crystal substance (mass fraction, %)

TFe	K	Si	Zn	Ca	Al
0	36.91	0	0	4.3	0
Na	Mg	Pb	F^-	Cl^-	SO_4^{2-}
5.27	0	0	0.1	37.3	16.85

some time the dominant factor of leaching rate was no longer the temperature, but the amount of soluble potassium on the dust surface. The XRD patterns of the leaching residues at the different leaching temperatures are shown in Fig. 9. The main components of the leaching residues were Fe_2O_3 and Fe_3O_4, with almost no diffraction peaks of KCl and NaCl presented. It is believed that the potassium was almost leached out of the dusts.

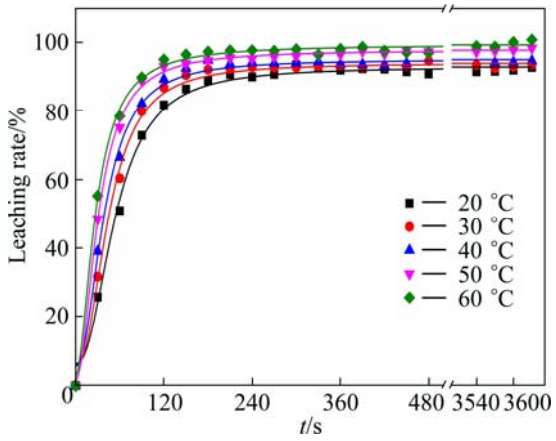

Fig. 8 Effect of temperature on leaching rate of K^+ with L/S ratio of 5:1 and stirring speed of 300 r/min

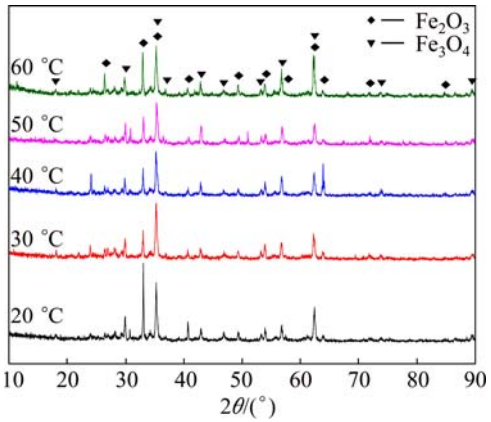

Fig. 9 XRD patterns of leaching residues at different leaching temperatures

A linear relationship obtained by plotting $1-(1-a_t)^{1/3}$ with leaching time t (Fig. 10(a)) and plotting ln$k$ with $-1/(RT)$ (Fig. 10(b)). This suggests that this leaching process can be perceived as the dissolution of the dissolvable constituents in the sintering dust, such as KCl

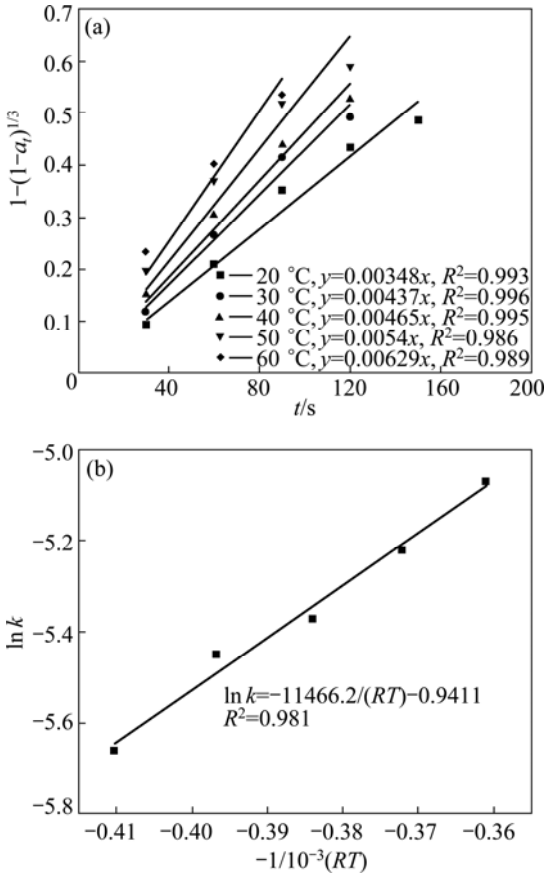

Fig. 10 Plots of $1-(1-a_t)^{1/3}$ vs time t at different temperatures (a) and ln$k$ vs $-1/(RT)$ (b)

and K_2SO_4, and the leaching rate is controlled by external diffusion. By the Arrheniu formula, the equation between leaching rate constant (k) and temperature (T) is written as $\ln k=-11466.2/(RT)-0.9411$.

The correlation coefficient R^2 is 0.981 and the calculated apparent activation energy (E_a) is 11.4662 kJ/mol. So, it is convinced that the water leaching process of sintering dusts conforms to the external diffusion model. Therefore, the leaching speed and the leaching rate of K^+ can be improved by increasing the concentration of the leaching solution and temperature, and by decreasing the grain size of sintering dust.

The leaching process of the sintering dust can be seen as a dissolution process of the soluble materials and a crushing process of the agglomerate particles. In the previous leaching experiments, dust particles were agglomerated together; with stirring continuing, the soluble materials were dissolved into the leaching solution and the agglomerated dust particles were crushed and scattered in the leaching solution. The crush and scatter processes are shown in Fig. 11. Comparison with the SEM image of the sintering dust before water leaching (Fig. 11(a)), the particle sizes are smaller and dispersed more uniformly after water leaching (Fig. 11(b)).

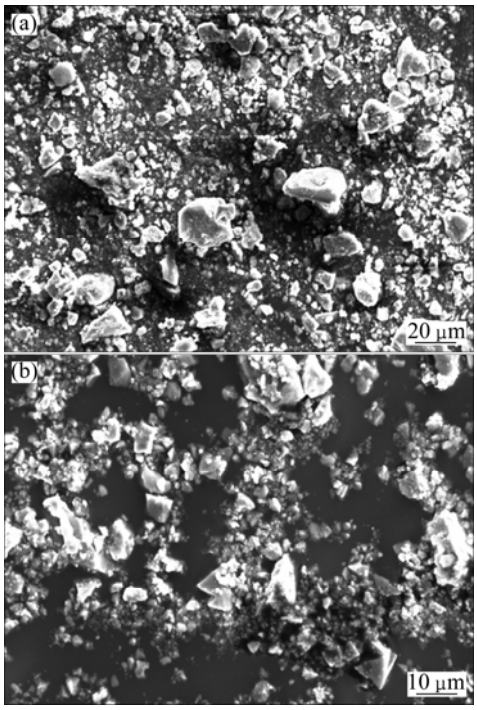

Fig. 11 SEM images of sintering dust before (a) and after (b) water washing

3.5 Measures of intensified leaching

3.5.1 Effect of stirring speed

The effect of the stirring speed on the leaching rate of K^+ of sintering dust in water (L/S was 5:1, mL/g) was investigated at 20 °C using the stirring speed of 200−500 r/min for 60 min. The results in Fig. 12 shows that the stirring speed influences the leaching speed and leaching rate of potassium. With a low stirring speed, dust particles tended to agglomerate together because the specific surface was large and the surface activation energy was high. Besides, a small amount of air might be adsorbed on the surface of dust particles, forming a relatively stable air film, which could prevent dust particles from being wetted and decrease the bulk density of dust particles, making the particles floating on the surface of water.

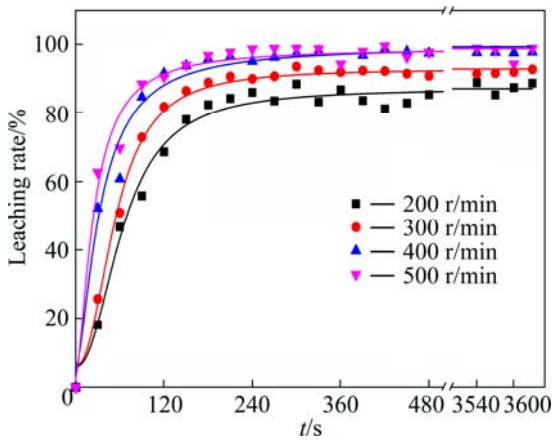

Fig. 12 Effect of stirring speed on leaching rate of K^+ of leaching solution with L/S of 5 mL/g at 20 °C

The pictures of the leaching experiments with stirring for 1 h at different speeds are shown in Fig. 13. It was found that the higher the stirring speed, the less the amount of dust floating on the water surface. The leaching situation at 200 r/min is shown in Fig. 13(b). A certain amount of dust, encapsulated with an air film, was found floating on the water, which probably was a reason for the low leaching rate of potassium in this case. Figures 13(d) and (e) show the pictures of the cases of 400 and 500 r/min, respectively. With these relatively faster stirring speeds, almost no dust but a certain number of stable air bubbles were found floating on the surface of water. For a better control of the leaching process, these air bubbles should be avoided whenever possible by choosing a suitable stirring speed.

3.5.2 Effect of liquid−solid ratio

The previous studies [6,13,15,16] proved that, the larger the liquid−solid ratio was, the faster and more complete the potassium was leached out. However, the large L/S ratio may increase the cost of the crystallization process. So it is necessary to choose an appropriate L/S ratio. The effect of the recycle times of the leaching solution on the leaching rate of potassium is shown in Figs. 14−18. In this experiment, the leaching time was set at 1 h, at beginning the first 20 g dust was leached with a fresh 100 mL water and the results of leaching rates for the dusts with fresh water were marked as 5:1, then, after filtration, the filtrate was recycled once for leaching of another 20 g dust. The result marked +1 means that the filtrate was recycled once, and so does +3 as well as +5 respectively represent the filtrate solution was reused three and five times. Obviously, the more times the solution has been recycled, the lower the leaching rate could be achieved, and the longer the leaching equilibrium time was. It is attributed that the concentrations of K_2SO_4 and $CaSO_4$ in leaching solution increased after recycle, and a double salt of $K_2Ca(SO_4)_2{\cdot}2H_2O$ precipitated [22,23]. The XRD diffraction peaks of the double salt $K_2Ca(SO_4)_2{\cdot}2H_2O$ were found in the residues of +3 and +5 (Fig. 15) and the SEM-EDS mapping distribution of K, Ca, S and O in Fig. 17 are as the same as those in Fig. 18, proving the existence of $K_2Ca(SO_4)_2{\cdot}2H_2O$ in the residues.

4 Conclusions

1) ICP-AES, XRD and SEM-EDS results show that K in the ESP dust is mostly present in the form of KCl, which is easy to be separated from other elements, such as Fe and C.

2) The total yield of K−Na vaporized crystalline salt is 18.56%, in which the mass fractions of KCl, NaCl,

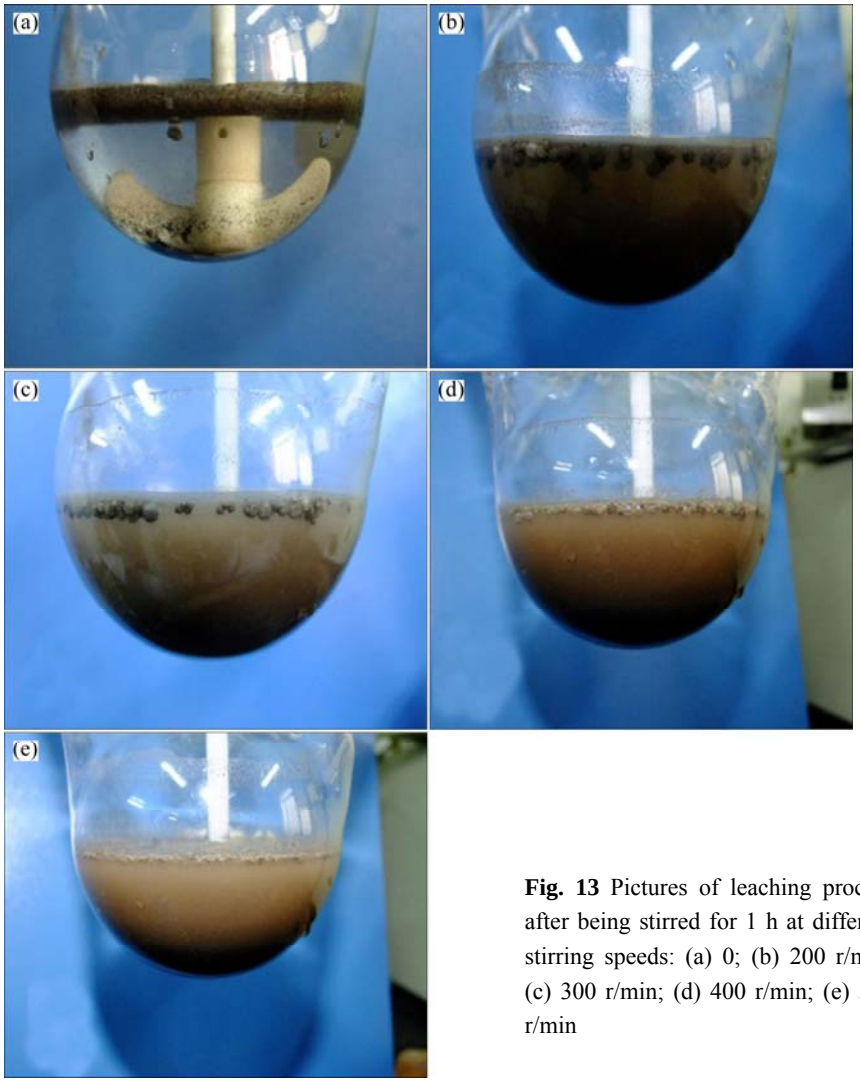

Fig. 13 Pictures of leaching process after being stirred for 1 h at different stirring speeds: (a) 0; (b) 200 r/min; (c) 300 r/min; (d) 400 r/min; (e) 500 r/min

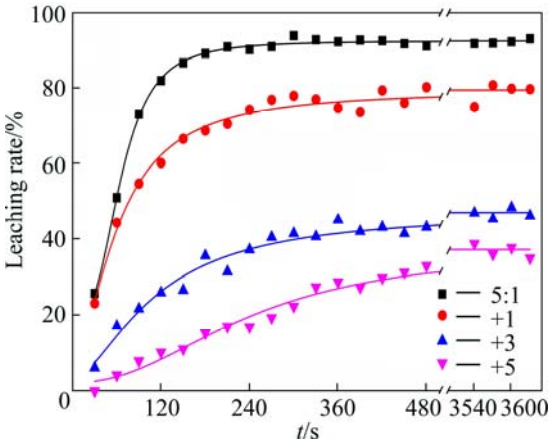

Fig. 14 Effect of recycle number of leaching solution on leaching rate of K^+

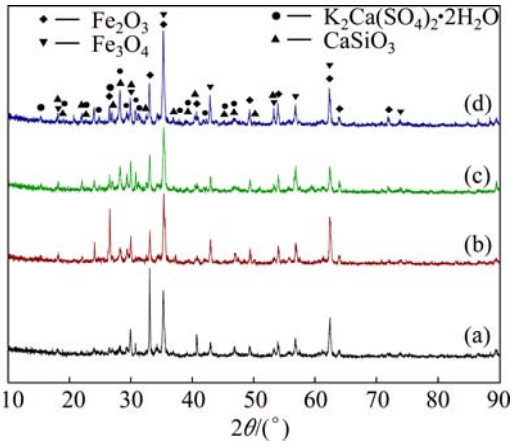

Fig. 15 XRD patterns of leaching residual: (a) First leaching; (b) Leaching solution recycling one times; (c) Leaching solution recycling three times; (d) Leaching solution recycling five times

$CaSO_4$ and K_2SO_4 are about 61.21%, 13.40%, 14.62% and 10.86%, respectively.

3) The leaching process of the ESP dust conforms to the external diffusion control model, $1-(1-a_t)^{1/3}=\exp[-11466.2/(RT)-0.9411]t$, and the activation energy (E_a) is 11.4662 kJ/mol. The leaching speed and leaching rate can be improved by increasing stirring speed, leaching temperature and liquid−solid ratio.

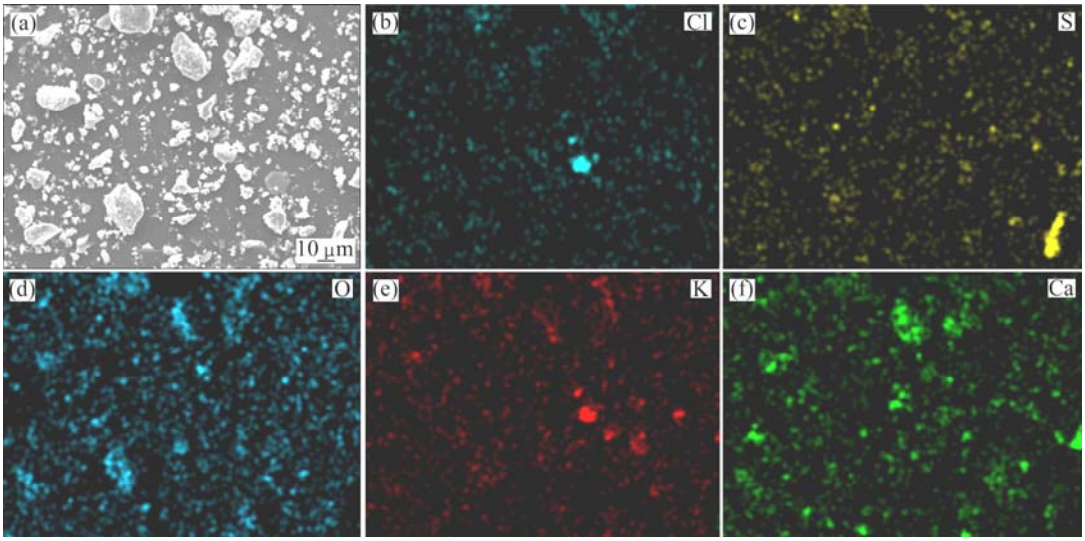

Fig. 16 SEM image (a) and EDS mapping (b, c, d, e, f) of leaching residual +1

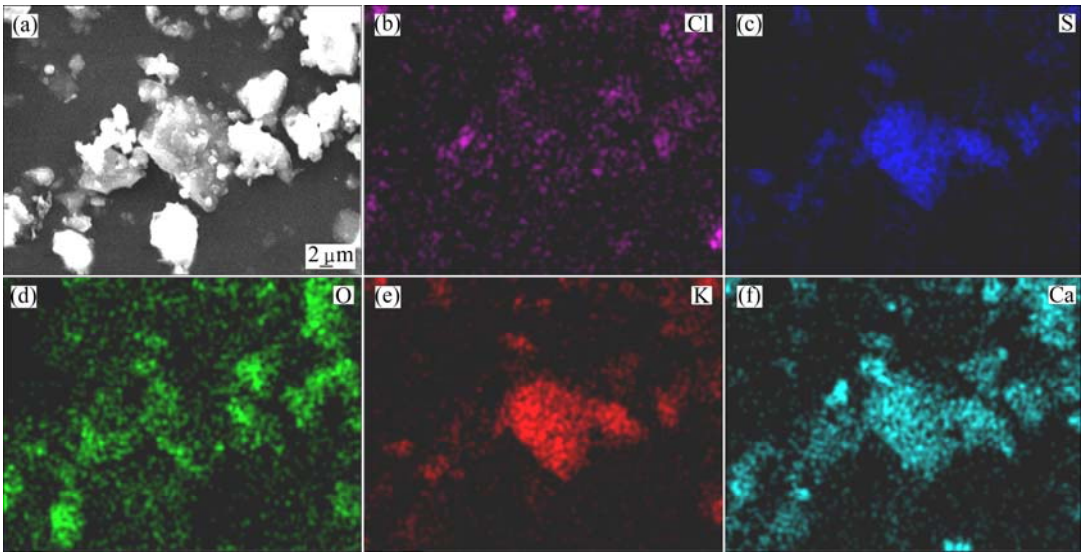

Fig. 17 SEM image (a) and EDS mapping (b, c, d, e, f) of leaching residual +3

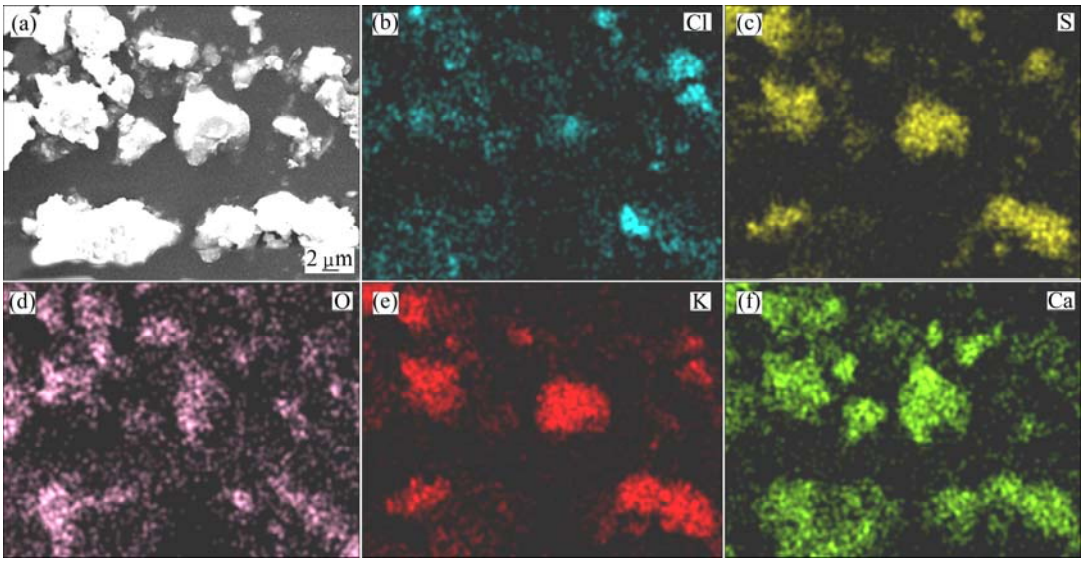

Fig. 18 SEM image (a) and EDS mapping (b, c, d, e, f) of leaching residual +5

4) The leaching speed and the leaching rate of K^+ increase with the increasing leaching temperature. There is a a significant influence on the leaching rate by stirring speed, which should be controlled not less than 300 r/min to ensure a good leaching rate of potassium. Due to a notable reduction in the leaching rate of the dust when used a recycled filtrate, it is advised that the leaching solution should not be recycled.

References

[1] BAO Rong-hua. China should adopt various countermeasures with the intensification of the monopoly on world-wide potash industries [J]. Land and Resources Information, 2012(7): 26−28. (in Chinese)

[2] Sina Finance [EB/OL]. [2012−11−29]. http://finance.sina.com.cn/nongye/nygd/ 20121129/112713840307.shtml. (in Chinese)

[3] WANG Jie. The lowest price in the world: China won the import contract for potash [N]. 21st Century Business Herald, 2012−03−22 (17). (in Chinese)

[4] SONG Peng-sheng, LI Wu, SUN Bai, NIE Zhen, BU Ling-zhong, WANG Yun-sheng. Recent development on comprehensive utilization of salt lake resources [J]. Chinese Journal of Inorganic Chemistry, 2011, 27(5): 801−815. (in Chinese)

[5] NIE Zhen, BU Ling-zhong, LIU Jian-hua, WANG Yun-sheng, ZHEN Mian-ping. Status of potash resources in salt lake and progress in potash technologies in China [J]. Acta Geoscientica Sinica, 2010, 31(6): 869−874. (in Chinese)

[6] ZHANG Fu-li, PENG Cui, GUO Zhan-cheng. Recovery of potassium chloride from sintering dust of ironmaking works [J]. Environmental Engineering, 2009, 27(S1): 337−340. (in Chinese)

[7] MU Ji-yao. Alkali metals in the blast furnace [M]. Beijing: Metallurgical Industry Press, 1992: 12−15. (in Chinese)

[8] TSAI J H, LIN K H, CHEN C Y, DING J Y, CHOA C G, CHIANG H L. Chemical constituents in particulate emissions from an integrated iron and steel facility [J]. Journal of Hazardous Materials, 2007, 147(1−2): 111−119.

[9] DUTRA A J B, PAIVA P R P, TAVARES L M. Alkaline leaching of zinc from electric arc furnace steel dust [J]. Minerals Engineering, 2006, 19(5): 478−485.

[10] BRUCKARD W J, DAVEY K J, RODOPOULOS T, WOODCOCK J T, ITALIANO L. Water leaching and magnetic separation for decreasing the chloride level and upgrading the zinc content of EAF steelmaking baghouse dusts [J]. International Journal of Mineral Processing, 2005, 75(1−2): 1−20.

[11] ORHAN G. Leaching and cementation of heavy metals from electric arc furnace dust in alkaline medium [J]. Hydrometallurgy, 2005, 78(3−4): 236−245.

[12] PICKLES C A. Thermodynamic modelling of the formation of zinc–manganese ferrite spinel in electric arc furnace dust [J]. Journal of Hazardous Materials, 2010, 179(1−3): 309−317.

[13] PENG Cui, GUO Zhan-cheng, ZHANG Fu-li. Existing state of potassium chloride in agglomerated sintering dust and its water leaching kinetics [J]. Transactions of Nonferrous Metals Society of China, 2011, 21(8): 1847−1854.

[14] The crude steel production of China is expected to be 720 million tons in 2012 [EB/OL]. [2012−11−13]. http://www.askci.com/news/201211/13/17202999.shtml. (in Chinese)

[15] PENG Cui, GUO Zhan-cheng, ZHANG Fu-li. Discovery of potassium chloride in the sintering dust by chemical and physical characterization [J]. ISIJ International, 2008, 48: 1398−1403.

[16] PENG Cui, ZHANG Fu-li, GUO Zhan-cheng. Separation and recovery of potassium chloride from sintering dust of ironmaking works [J]. ISIJ International, 2009, 49: 735−742.

[17] GUO Zhan-cheng, PENG Cui, ZHANG Fu-li, PAN Zhao-bin. Utilization of sintering dust of iron and steel enterprise for producing potassium chloride: China, 200810101269 [P]. 2008−03−03. (in Chinese)

[18] LUO Guo-ping, SUN Guo-long, ZHAO Yan-xia, ZHANG Xue-feng, HAO Zhi-zhong, WU Sheng-li. Experimental study on basic sintering characteristics of Baogang iron ore powder [J]. The Chinese Journal of Process Engineering, 2008, 8(S1): 198−204. (in Chinese)

[19] FANG Zhao-heng. Leaching [M]. Beijing: Metallurgical Industry Press, 2007: 7−9. (in Chinese)

[20] LI Hong-gui. Science of hydrometallurgy [M]. Changsha: Central South University Press, 2002: 69−81. (in Chinese)

[21] LEVENSPIEL O. Chemical reaction engineering [M]. New York: Wiley, 1972.

[22] YANG Xin-ya, YU De-gao, WANG Jin-hua. Research on hydration mechanism of calcium sulfate anhydrite activated by potassium sulfate [J]. Journal of Shenyang Jianzhu University, 2008, 24(1): 104−107. (in Chinese)

[23] GREENBERG J P, MOLLER N. The prediction of mineral solubilities in natural waters: A chemical equilibrium model for the Na−K−Ca−Cl−SO_4−H_2O system to high concentration from 0 to 250 °C [J]. Geochimica et Cosmochimica Acta, 1989, 53: 2503−2518.

烧结电除尘灰中钾盐的回收及其浸出动力学

詹 光，郭占成

北京科技大学 钢铁冶金新技术国家重点实验室，北京 100083

摘 要：为了研究烧结电除尘灰中回收钾盐的强化浸出措施，使用 ICP−AES、SEM−EDS 和 XRD 分析技术对除尘灰的表面和内部形态，特别是钾盐的赋存形式进行分析。结果表明，该电除尘灰的主要成分是铁氧化合物，在其表面裸露吸附着一定含量的 KCl 晶体。水浸实验表明，该粉尘中的 KCl 可以通过水浸出、蒸发结晶的方式回收，其收率为 18.56%。结晶产物的分析结果表明，KCl 占 61.21%，NaCl 占 13.40%，$CaSO_4$ 占 14.62%，K_2SO_4 占 10.86%。其水浸出动力学符合外扩散控制模型控制。强化浸出实验表明，提高浸出温度、加强搅拌、增加液固比等措施可以提高钾盐的浸出率和浸出速率。

关键词：钾盐；烧结粉尘；浸出动力学；强化浸出

(Edited by Hua YANG)